Peer Review File

Broadband and parallel multiple-order optical spatial differentiation enabled by Bessel vortex modulated metalens

REVIEWER COMMENTS

Reviewer #1 (Remarks to the Author):

My reviewing commments have been attatched with a separate file.

[**Editorial note**: Please see the next page for reviewer #1’s comments.]

1. Although the authors have cited reference 41, there are other methods that achieve multiple-order differentiation using a single device that have not been cited (Laser Photonics Rev. 2022, 16, 2200230).

2. In Supplementary Section 1, δll' in the equation $\int_0^{2\pi} \exp(il\varphi)\exp(il'\varphi)\,\mathrm{d}\varphi = 2\pi\delta_{ll'}$ is not defined. And if $\delta_{ll'} = \begin{cases} 1 & (l = l') \\ 0 & (l \neq l') \end{cases}$, the equation should be $\int_0^{2\pi} \exp(il\varphi)\exp(-il'\varphi)\,\mathrm{d}\varphi = 2\pi\delta_{ll'}$. And the following Eqs. (S5-S8) should also be checked.

3. φ_k in Eqs. (S6-S8) is not defined.

4. The figures in Fig. S11 do not show one-four peaks along the radial direction like those in Fig. 4. Is the difference from the smooth edge of circular-shaped amplitude object in Fig. S11? The results of the objects used in Fig. S11, S12 can also be added. What is the meaning of the 'wide edge'? And the diameters of the objects in Figs. S11, S12 are about 70 nm, which are much smaller than the wavelength. Do not the small diameters affect the uniformity in amplitude and phase profiles along the radial direction of the objects in Figs. S11, S12, respectively?

5. The period of the super-pixel is $2P = 500$ nm, which is close to the wavelengths in the visible. Will it affect the device's broadband performance and result in nonideal isotropic results like Fig. 4 even in the simulations?

6. 'Figure 5d' in the 223rd line in the main text should be 'Figure 5e'.

7. The experimental results in Figs. 4 and 5 are not very ideal, especially for the higher-order cases.

Reviewer #2 (Remarks to the Author):

In this paper, a Bessel vortex-modulated metasurface composed of a singlet complex amplitude metasurface is proposed and experimentally proven. By presetting the order of the Bessel vortex, the multiorder radial differential operation can be performed in a wide band, indicating the advantages of the proposed device in parallel processing. This work is very interesting and can be seen as a significant advancement in Optical Analogue Computing. It is unquestionable that this work can inspire great interest among researchers in the field of optical spatial differentiation. I recommend the acceptance of this interesting paper after the authors have addressed the following concerns.

1. In this paper, the phase of the Bessel vortex beam with topological charge L on the metasurface can achieve differential operation of order L. Can the phases of other vortex beams, such as Laguerre Gaussian vortex beams, achieve similar effects?

2. In Figure 1c-f and Figure 2j-m, differential operations of higher order have larger differential intervals (range of k wave vectors). What‘s the reason for this?

3. Is it necessary to precisely align the center of the BVML structure with the center of the illumination beam (sample) during the experiment? If the centers of the two are slightly shifted, will the differential effect be greatly affected?

4. In Figure 1a, the first-, second-, third-, and fourth-order differential images appear at different focal planes of the metasurface. This is inconsistent with Figure 5a. The authors should revise the two images.

5. It is not very formal that all the references are cited in the section Introduction. There is no reference appearing in the other sections.

6. It is better that the authors make more standard comparisons between this work and that in Reference 41. In Reference 41, a multiple-order analogue spatial differentiator was also realized with the same optical element, where the incident beam can strike any position of the dielectric multilayer. It is also easier to fabricate dielectric multilayers than

metasurfaces. The two works involve different mechanisms: one is based on the nonlocality of the dielectric multilayer, and the other is based on the unique phase properties of the metasurface.

Reviewer #3 (Remarks to the Author):

The authors propose an optical edge detection system with Bessel vortex modulated metalens. By designing a metalens with Bessel vortex modulated geometric phases, specific spectrum transfer functions are realized to enable multiple-order optical spatial and wide-band edge detection. I think that the results are quite interesting, and the combination of several different order could be useful in some bio-image applications. Below there are some comments for the authors' consideration.

1. The proposed optical differentiation strongly relays the orthogonal polarizations between the incident and the output field, and the geometric phase. However, the previous differentiation works on these topics are not introduced, such as Physical Review Applied 11, 034043 (2019), Advanced Photonics 2, 016001 (2020), Nature Communications 12, 680 (2021).

2. It seems that the Objective in Fig. 3a operates as the Fourier lens. In this case, the CCD records the spatial frequency domain of the differentiation image, instead of the real-space.

3. In comparison with Fig. 3(c-e), Fig. 3f shows the degraded performance for fourth-order differentiation, which needs more detailed explanation and discussion.

Reviewer #4 (Remarks to the Author):

This manuscript proposes a metasurface design for optical spatial differentiation. Combining the phases of a vortex beam and a lens, the metasurface can achieve almost any order diffraction by using the corresponding topological charge of the vortex phase. The authors also give experimental demonstrations of the device. The concept is given clearly and the idea is interesting. However, in my opinion, some questions need to be addressed and more details should be provided before it can be further evaluated.

1. According to the derivation of the authors, the differential function of the metasurface is based on the small argument approximation. Thus, the application scope of the method should be discussed in this study. Since the variable of the Bessel function is related with \xi, f/R, kr/k0, how these values will influence the function should be studied. What is the spatial frequency range of the image used in the study is also suggested to be given.
2. According to the principle of the manuscript, tl(kr) is proportional to (kr/k0)^l. Does it mean the differentiation is only in the radial direction, not in the angular direction?
3. To highlight the novelty of this work, I suggest the authors give a comparison on the mechanism of this method and those of other works of spatial differentiation.
4. Is PB phase modulation required to realize the metalens?
5. ωl is the corresponding weight of each channel in Eq. (4). What is it for the 5 channels? How to determine and balance this value for various channels.
6. A photo of the unstained limewood stem cell sample in the optical path is suggested to be given.
7. Please give physical explanation for “higher-order differential operations have greater advantages in blocking low- to mid-frequency components” in Line 219-220.
8. It should be Fig.5e in Line 223.
9. To apply the differentiation function of the method, the authors use the metalens for realizing edge detection. Are there any other applications for high order optical differentiation?

Response to the referees' comments:

Reviewer #1 (Remarks to the Author):

1. Although the authors have cited reference 41, there are other methods that achieve multiple order differentiation using a single device that have not been cited (Laser Photonics Rev. 2022, 16, 2200230).

Authors Reply: Sincere thanks for this constructive comment. We updated the manuscript by adding this reference. The relevant description has also been added to Page 2 and 11 in the revised manuscript as follows:

"Up to this point, most planar meta-optics have been limited to low-order differential operations, such as the first- or second-order [14-24, 32-44].

"[32] Zhao, M., Liang, X., Li, J., Xie, M., Zheng, H., Zhong, Y., Yu, J., Zhang, J., Chen, Z., Zhu, W. Optical phase contrast microscopy with incoherent vortex phase. *Laser Photon. Rev.* **16**, 2200230 (2022)."

2. In Supplementary Section 1, δll' in the equation $\int_0^{2\pi} \exp{(il\varphi)} \exp{(il'\varphi)} \mathrm{d}\varphi = 2\pi\delta_{ll'}$ is not defined. And if $\delta_{ll'} = \begin{cases} 1 & (l = l') \\ 0 & (l \neq l') \end{cases}$, the equation should be $\int_0^{2\pi} \exp{(il\varphi)} \exp{(-il'\varphi)} \mathrm{d}\varphi = 2\pi\delta_{ll'}$. And the following Eqs. (S5-S8) should also be checked.

Authors Reply: We thank the reviewer for pointing out this problem and apologize for the unclear definition. Following the reviewer's suggestion, we have added this precise definition to line 40-42 of the revised supplementary materials and corrected the Eqs. (S5-S8).

3. φ_k in Eqs. (S6-S8) is not defined.

Authors Reply: We thank the reviewer for pointing out this problem. We define the polar coordinates of the spatial frequency domain of the image as (k_r, φ_k) to match the polar coordinates, (ρ, ϕ), of the image plane. The related description has been added in the page 3 of the revised supplementary materials.

4. The figures in Fig. S11 do not show one-four peaks along the radial direction like those in Fig. 4. Is the difference from the smooth edge of circular-shaped amplitude object in Fig. S11?

The results of the objects used in Fig. S11, S12 can also be added. What is the meaning of the 'wide edge'? And the diameters of the objects in Figs. S11, S12 are about 70 nm, which are much smaller than the wavelength. Do not the small diameters affect the uniformity in amplitude and phase profiles along the radial direction of the objects in Figs. S11, S12, respectively?

Authors Reply: We thank the reviewer for raising these insightful points. Firstly, we would like to state the concept of "edge," which mainly results in the difference between Fig. S11, S12, and the former simulation figures. We assume that both the background and the inside of the objects are uniform in amplitude and phase without loss of generality, and the changes in the amplitude or phase of the transmitted field indicate the edges of the objects. As the proposed Bessel vortex modulated metalens (BVML) performs the radial differential operations, we can observe that the number of the peaks shown at the edge of the differential image equals the order of the BVML and the order of the differential operation if the object edge shows a step function against the background whether in amplitude or phase terms. In contrast, when the edge shows a gradual transition from the background to the inside of the object over a long distance, which is described as the "wide edge" in the SI, the number of peaks shown at the edge of the output image tends not to equal the order of the differential operation conducted by the BVML. Therefore, the figures in Fig. S11 do not show four peaks along the radial direction since the edge cannot be approximated as a step function as it changes smoothly over a relatively large radial distance in the phase term. The results of the objects used in Fig. S11 and S12 have also been added to page 16 of supplementary materials. Secondly, we are terribly sorry to note that the label of the horizontal coordinate should be "position (μm)" rather than "position (nm)." Whether the edge changes smoothly or not, the BVML cannot distinguish the object whose size is much smaller than its resolution.

5. The period of the super-pixel is 2P = 500 nm, which is close to the wavelengths in the visible. Will it affect the device's broadband performance and result in nonideal isotropic results like Fig. 4 even in the simulations?

Authors Reply: Many thanks for the comment. The period of the super-pixel mainly determines the maximum deflection angle provided by the metasurface and, therefore, the maximum numerical aperture of the device. For the modulated incident wavelength of 490nm-633nm, the period of super-pixel can provide the maximum in-plane wavevector as $6.28 \times 10^6\ rad/m$ and the maximum deflection angle as $0.51\ rad$, corresponding to a maximum numerical aperture of 0.49. For the BVMLs proposed in this paper, the numerical aperture is designed as 0.45, which is less than the upper limit of the numerical aperture provided by the period and thus can satisfy the requirement of the BVML to achieve the broadband differential operation mentioned in the paper. The aberrations in the uncollimated optical path mainly cause the imperfect results in Figure 4. We have made some optimizations to this problem, and the corresponding updated results of Figure 4 are also presented in the seventh answer below.

6. 'Figure 5d' in the 223rd line in the main text should be 'Figure 5e'.

Authors Reply: We thank the reviewer for pointing out this problem. It has been corrected to line 225 of the revised manuscript.

7. The experimental results in Figs. 4 and 5 are not very ideal, especially for the higher-order cases.

Authors Reply: Many thanks for the valuable comment. After careful analysis, we found that the imperfections in Figure 4 are mainly due to the aberrations of the imaging system, which come from the misalignment and slight tilt of the experimental optical path. These results have been optimized and updated in Figure 4 of the revised manuscript, as shown in Figure R1 below. In addition, the synchronization processing of multi-order differential operations is realized by angle multiplexing multiple information channels with different deflection phase profiles. The field of view of the device is limited, so the aberration of each output channel deteriorates the edge results of the image in Figure 5. This situation can be alleviated in the future by optimizing the field of view for each information channel.

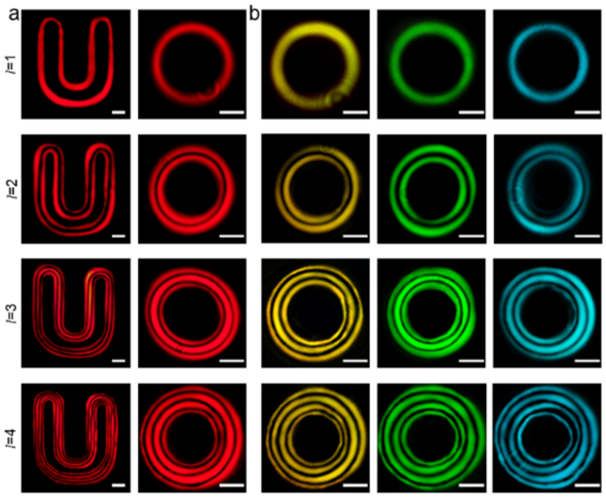

Figure R1 | Experimental broadband differential imaging results of amplitude objects. **a** The first- to fourth-order differential imaging results of the U-shaped and circular objects at the wavelength of 633 nm. **b** The first- to fourth-order differential imaging results of the circular object at the wavelengths of 580, 532, and 490 nm, respectively. Scale bars: 10 μm.

Reviewer #2 (Remarks to the Author):

In this paper, a Bessel vortex-modulated metasurface composed of a singlet complex amplitude metasurface is proposed and experimentally proven. By presetting the order of the Bessel vortex, the multiorder radial differential operation can be performed in a wide band, indicating the advantages of the proposed device in parallel processing. This work is very interesting and can be seen as a significant advancement in Optical Analogue Computing. It is unquestionable that this work can inspire great interest among researchers in the field of optical spatial differentiation. I recommend the acceptance of this interesting paper after the authors have addressed the following concerns.

Authors Reply: We would like to thank the referee for reviewing the manuscript and giving positive comments.

1. In this paper, the phase of the Bessel vortex beam with topological charge L on the metasurface can achieve differential operation of order L. Can the phases of other vortex beams, such as Laguerre Gaussian vortex beams, achieve similar effects?

Authors Reply: We thank the reviewer for making an insightful point. In this work, the differential processing capability of the proposed devices BVMLs mainly relies on its coherent transfer function $t_l(k_r) \propto J_l(\alpha f k_r/k_0) \propto (\alpha f k_r/k_0)^l$ around $k_r = 0$, which is ensured by the complex amplitude modulation of Bessel vortices and the asymptotic behavior of the Bessel function with near-zero variable. Then according to the reviewer's comments, we simulate and fit the coherent transfer function of the Laguerre Gaussian vortex modulated lens. We find that the coherence transfer function of Laguerre Gaussian vortex modulated lenses of different orders also exhibits a corresponding exponential dependence in a specific spatial frequency range, as shown in the first row of Figure R2 below. Therefore, the Laguerre Gaussian vortex modulated lens can indeed perform differential operations of the corresponding order, which has also been verified by the numerical simulation results of the circular aperture object, as shown in the second row of Figure R2 below.

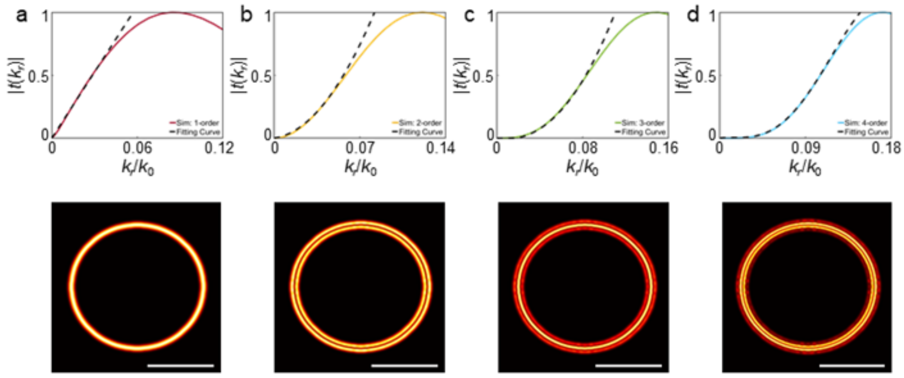

Figure R2 | Coherence transfer function and numerically simulated differential images formed by the Laguerre Gaussian vortex modulated lens. **a** The first-order, **b** The second-order, **c** The third-order, **d** The fourth-order. Scale bar: 40 μm.

2. In Figure 1c-f and Figure 2j-m, differential operations of higher order have larger differential intervals (range of k wave vectors). What's the reason for this?

Authors Reply: Thanks for the comment. The coherent transfer function of the proposed BVML in the spatial frequency domain can be derived as $t_l(k_r) \propto J_l(\alpha f k_r/k_0)$. Therefore, the reason why the higher order differential operation has a large differential interval should be attributed to the properties of Bessel functions themselves. To investigate the effective scope of the asymptotic form $J_l(z) \sim \frac{1}{\Gamma(l+1)}\left(\frac{z}{2}\right)^l$, the polynomial fitting results are given in Figure R3 below. As can be seen from the simulation results, the higher order Bessel functions have a broader scope of the variable values to satisfy the asymptotic form. Therefore, the differential operations of higher order have larger differential intervals (range of k wave vectors).

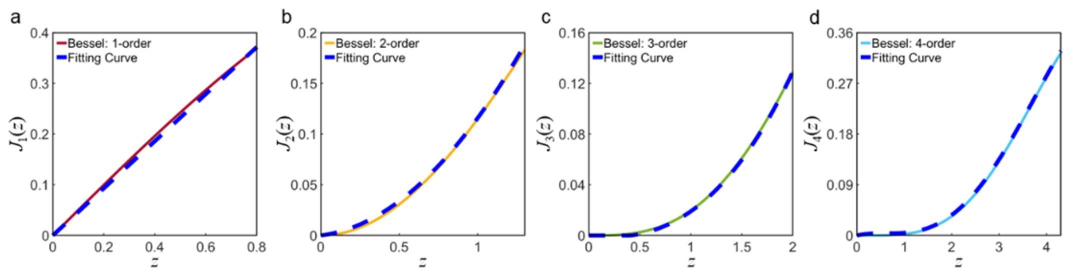

Figure R3 | The simulated Bessel functions of different orders and the corresponding polynomial fitting curves of the same order. **a** The first-order, **b** The second-order, **c** The third-order, **d** The fourth-order.

3. Is it necessary to precisely align the center of the BVML structure with the center of the illumination beam (sample) during the experiment? If the centers of the two are slightly shifted, will the differential effect be greatly affected?

Authors Reply: Many thanks for the comment. In this work, the differential processing capability of the proposed devices BVMLs is mainly enabled by its coherent transfer function $t_l(k_r) \propto (\alpha f k_r/k_0)^l$. From the point of view of the differential operation, a slight shift of the center does not change the transfer function of the device and, therefore, does not affect the differential processing effect of the system. However, from an imaging perspective, the significant shift of the center can lead to the imaging system's aberration, which will deteriorate the effect of differential processing. This conclusion has also been verified by the simulated third-order differential imaging results of the object with different offsets from the center of the BVML, as shown in Figure R4 below. The situation can be alleviated in the future by optimizing the field of view and aberration of the devices.

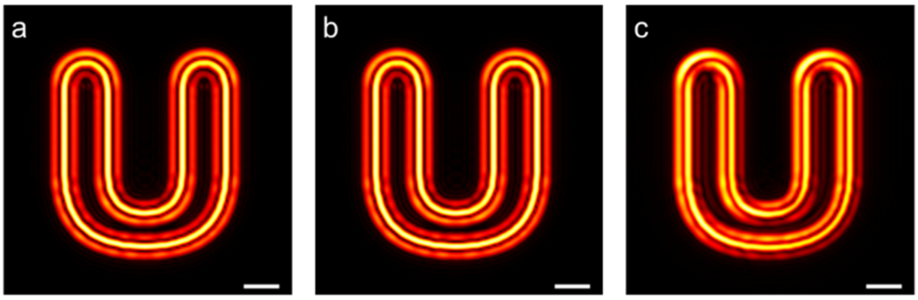

Figure R4 | Numerically simulated third-order differential images with different offsets from the center of the BVML. **a** 0 μm offset, **b** 50 μm offset, **c** 200 μm offset. Scale bar: 30 μm.

4. In Figure 1a, the first-, second-, third-, and fourth-order differential images appear at different focal planes of the metasurface. This is inconsistent with Figure 5a. The authors should revise the two images.

Authors Reply: We thank the reviewer for pointing out these problems. We apologize for the misguidance in plotting the first-, second-, third-, and fourth-order differential images at different focal planes of the metasurface in Figure 1a. The original schematic tends to illustrate that the metasurface device modulates the incident object light field and outputs a lth-order differential image at the imaging plane according to the order of the Bessel vortex encoded in its profile. Since there is no principal limit to the order of the BVML, the device can accomplish the first-, second-, third-, fourth-, or even higher-order spatial differential operation. Moreover, the schematic in Figure 5a expresses that we can realize synchronization processing of multi-order differential operations by adopting angle multiplexing of the mentioned BVML design. According to the reviewer's suggestion, the problem has been corrected by replacing the original Figure 1a with the new schematic as follows:

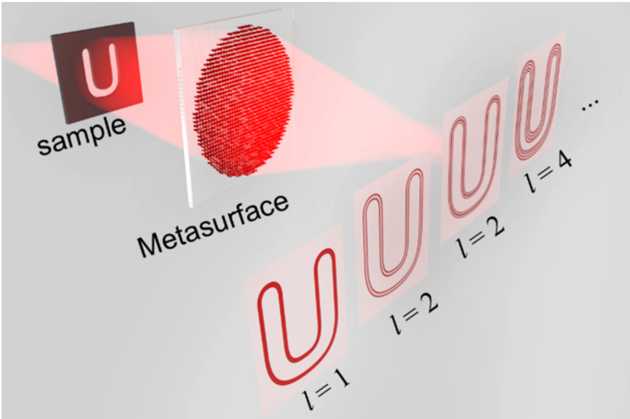

Figure R5 | Revised schematic of the proposed BVML based on a dielectric metasurface.

5. It is not very formal that all the references are cited in the section Introduction. There is no reference appearing in the other sections.

Authors Reply: We are very grateful to the reviewer for the valuable comment. According to the reviewer's suggestion, we updated the manuscript by citing more related literature in the Design and Fabrication section, as described in line 116-117 of the revised manuscript.

6. It is better that the authors make more standard comparisons between this work and that in Reference 41. In Reference 41, a multiple-order analogue spatial differentiator was also realized with the same optical element, where the incident beam can strike any position of the dielectric multilayer. It is also easier to fabricate dielectric multilayers than metasurfaces. The two works involve different mechanisms: one is based on the nonlocality of the dielectric multilayer, and the other is based on the unique phase properties of the metasurface.

Authors Reply: We agree with the reviewer's comment that the work in reference 41 is a novel approach to implement multi-order difference operations. It is indeed based on the nonlocality of the dielectric multilayer and is also easier to fabricate. In order to highlight these features, we have added relevant descriptions to line 48-51 in the revised manuscript, as follows:

“Based on the nonlocality of the dielectric multilayer, a multiple-order analog spatial differentiator is proposed to realize some higher-order differential operations, such as the third- or fourth-order [45]. The device offers significant advantages in terms of low-complex fabrication and low sensitivity to misalignment.”

Reviewer #3 (Remarks to the Author):

The authors propose an optical edge detection system with Bessel vortex modulated metalens. By designing a metalens with Bessel vortex modulated geometric phases, specific spectrum transfer functions are realized to enable multiple-order optical spatial and wide-band edge detection. I think that the results are quite interesting, and the combination of several different order could be useful in some bio-image applications. Below there are some comments for the authors' consideration.

Authors Reply: We would like to thank the reviewer for his/her time in reading and critiquing our manuscript, and for providing valuable feedback.

1. The proposed optical differentiation strongly relays the orthogonal polarizations between the incident and the output field, and the geometric phase. However, the previous differentiation works on these topics are not introduced, such as Physical Review Applied 11, 034043 (2019), Advanced Photonics 2, 016001 (2020), Nature Communications 12, 680 (2021).

Authors Reply: Sincere thanks for this constructive comment. We updated the manuscript by adding these references. The relevant description has also been added to Page 2 and 11 in the revised manuscript as follows:

"Up to this point, most planar meta-optics have been limited to low-order differential operations, such as the first- or second-order [14-24, 32-44].

"[33] Zhu, T., Lou, Y., Zhou, Y., Zhang, J., Huang, J., Li, Y., Luo, H., Wen, S., Zhu, S., Gong, Q., Qiu, M., Ruan, Z. Generalized spatial differentiation from the spin Hall effect of light and its application in image processing of edge detection. *Phys. Rev. Appl.* **11**, 034043 (2019).

"[34] Zhu, T., Huang, J., Ruan, Z. Optical phase mining by adjustable spatial differentiator. *Adv. Photonics.* **2**, 016001 (2020).

"[35] Zhu, T., Guo, C., Huangm J., Wang, H., Orenstein, M., Ruan, Z., Fan, S., Topological optical differentiator. *Nat. Commun.* **12**, 680 (2021)."

2. It seems that the Objective in Fig. 3a operates as the Fourier lens. In this case, the CCD records the spatial frequency domain of the differentiation image, instead of the real-space.

Authors Reply: Many thanks for the comment. We apologize for any confusion resulting from our experiment light path schematic. When the objective lens acts as a Fourier lens, the input and recording planes should be placed on the front and rear focal planes of the lens. However, in our work, the input differential images and recorded CCD are respectively placed on the object plane and the image plane of the objective lens, which are a pair of conjugate planes. Here, the objective lens serves to relay the differential image of the BVMLs output. Therefore, the CCD records the differential image magnified by the objective lens rather than the spatial frequency domain of the image.

3. In comparison with Fig. 3(c-e), Fig. 3f shows the degraded performance for fourth-order differentiation, which needs more detailed explanation and discussion.

Authors Reply: We thank the reviewer for pointing out this problem. Higher-order differential operations tend to have lower resolutions, as verified by the measured point spread function (PSF). The size of the observed test target in the resolution test chart is close to the resolution limit of the fourth-order BVML and may lead to degraded performance of Figure 3f. Moreover, we also found that the imperfections in Figure 3f may be caused by aberrations in the imaging system from misalignment and slight tilt of the experimental optical path. By optimizing the experimental optical path, Figure 3e and 3f have been updated in the revised manuscript, as shown in Figure R6 below.

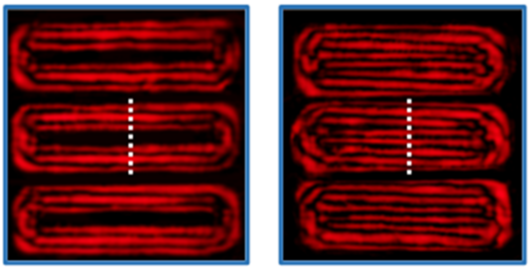

Figure R6 | Revised imaging results of the test target 5-4 formed through the third- and fourth-order BVMLs.

Reviewer #4 (Remarks to the Author):

This manuscript proposes a metasurface design for optical spatial differentiation. Combining the phases of a vortex beam and a lens, the metasurface can achieve almost any order diffraction by using the corresponding topological charge of the vortex phase. The authors also give experimental demonstrations of the device. The concept is given clearly and the idea is interesting. However, in my opinion, some questions need to be addressed and more details should be provided before it can be further evaluated.

Authors Reply: We would like to thank the reviewer for providing careful and constructive comments, which have helped improve the quality of the manuscript.

1. According to the derivation of the authors, the differential function of the metasurface is based on the small argument approximation. Thus, the application scope of the method should be discussed in this study. Since the variable of the Bessel function is related with \xi, f/R, kr/k0, how these values will influence the function should be studied. What is the spatial frequency range of the image used in the study is also suggested to be given.

Authors Reply: We thank the reviewer for raising these insightful points. To investigate the application scope of the differential operation of the metasurface based on the small argument approximation, we conducted numerical simulations to explore the spatial frequency response of the BVML. Firstly, we investigated the ranges of the variable z to satisfy the asymptotic form of the Bessel function as $J_l(z) \sim z^l$. The fitting curves for different order Bessel functions, as shown in Figure R7, reveal that lower order Bessel functions have a limited and relatively more minor range of the variable value to match the asymptotic form. This led us to the conclusion that the spatial frequency of the object should be limited to the effective spatial frequency range marked in Figure 1c-1f for the corresponding order differential operations. However, it's worth noting that the edge detection application does not impose a strict limit on the input spatial frequency. Furthermore, we carried out a simulation to discuss the parameters' effect on the spatial frequency range of the differential operation. We set different values for the variables α and f as $\alpha=\xi_{2,l}/R$ or $\alpha=\xi_{4,l}/R$, and $f=R$ or $f=2R$. The corresponding CTFs of different order l are shown in Figure R8. As can be seen from the simulation results, smaller values of f/R and $\xi_{n,l}$ tend to extend the effective spatial frequency range of the differential operation. At last, we calculated the spatial frequency ranges of the objects in Figure 4 by using the fast Fourier transform and presented the corresponding results in Figure R9. It is clear that their spatial frequencies are within the processing range of the metasurface.

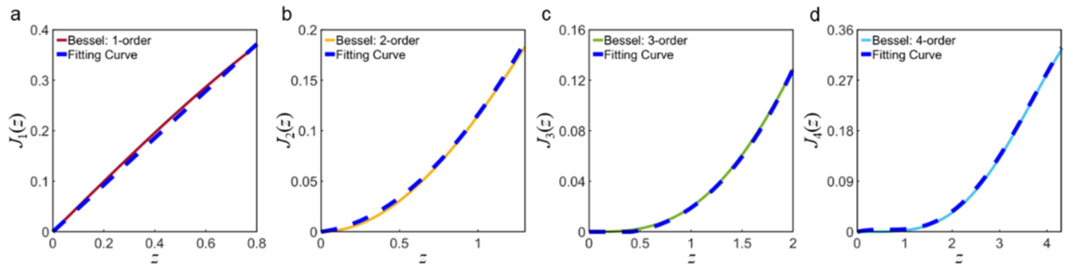

Figure R7 | The simulated Bessel functions of different orders and the corresponding polynomial fitting curves of the same order. **a** The first-order, **b** The second-order, **c** The third-order, **d** The fourth-order.

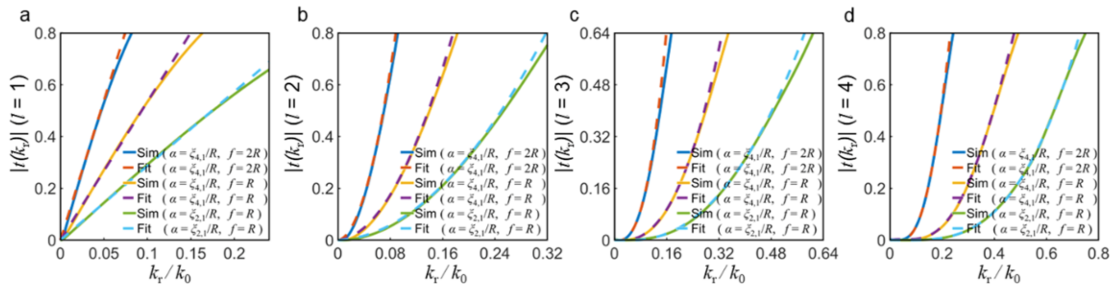

Figure R8 | The simulated CTF curves for different order BVMLs and the corresponding fitting curves using the form $|t(k_r)| = a|k_r|^l$. The abbreviation "Sim" has the full name of "Simulation". The abbreviation "Fit" has the full name of "Fitting". **a** The first-order, **b** The second-order, **c** The third-order, **d** The fourth-order.

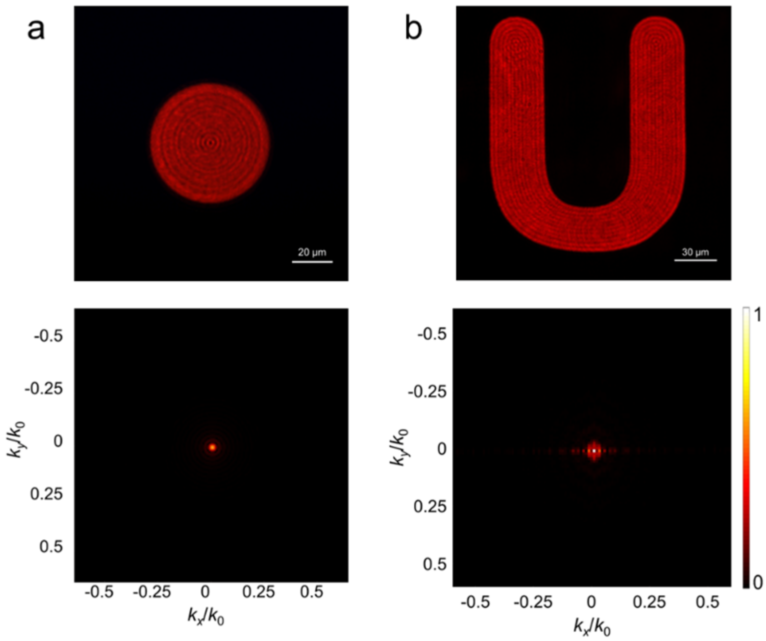

Figure R9 | Optical photographs and the corresponding spatial frequency ranges of the amplitude objects. **a** The circular aperture. **b** The U-shaped aperture.

2. According to the principle of the manuscript, $t_l(k_r)$ is proportional to (k_r/k_0)^l. Does it mean the differentiation is only in the radial direction, not in the angular direction?

Authors Reply: We fully concur with the reviewer's opinion that the differentiation only exists in the radial direction. According to the coherent transfer function and the asymptotic form of the Bessel function, we can obtain that the coherent transfer function fundamentally satisfies the form of $t_l(k_r) \propto (\alpha f k_r/k_0)^l$. Therefore, the proposed BVML only performs arbitrary order isotropic radial differential operation.

3. To highlight the novelty of this work, I suggest the authors give a comparison on the mechanism of this method and those of other works of spatial differentiation.

Authors Reply: We are very grateful to the reviewer for the constructive suggestion. To make more standard comparisons between our work and that in references, we added more detailed literature in the Introduction section on Pages 1-2 of the revised manuscript.

Various spatial differentiation works can realize spatial differential operation through the 4-*f* system [1-3], such as the incoherent vortex topological quadrupole in a thin uniaxial crystal [4], and the spin-optical and phase mining method by analyzing polarization states of reflected light from a dielectric interface [5-6]. Such differential devices [1-8] require a series of bulky optical elements to filter the light field.

Several compact optical differentiators based on nanophotonic materials have been developed to improve integration [9-20]. The compact meta-optics can integrate into the conventional microscopy system. However, most planar meta-optics can only perform low-order differential operations, such as the first- or second-order, without broadband response.

Based on the nonlocality of the dielectric multilayer, a multiple-order analog spatial differentiator is proposed to realize some higher-order differential operations, such as the third- or fourth-order [21]. The novel device offers significant advantages in terms of low-complex fabrication and low sensitivity to misalignment. However, this approach limits the broadband expansion and parallel processing capabilities of optical computations.

In contrast, we demonstrated a compact arbitrary order differentiator based on the metasurface with a broadband response and parallelism. Based on the unique PB phase property of the metasurface, we proposed a complex amplitude profile for a Bessel vortex modulated metalens (BVML). The BVML can perform multiple-order radial differential operations and enable parallel processing of different order differential operations in a broad frequency range.

[1] Abdollahramezani, S., Chizari, A., Dorche, A. E., Jamali, M. V., Salehi, J. A. Dielectric metasurfaces solve differential and integro-differential equations. *Opt. Lett.* **42**, 1197–1200 (2017).

[2] Huo, P., Zhang, C., Zhu, W., Liu, M., Zhang, S., Zhang, S., Chen, L., Lezec, H. J., Agrawal, A., Lu, Y. Q., Xu, T. Photonic spin-multiplexing metasurface for switchable spiral phase contrast imaging. *Nano Lett*. **20**, 2791–2798 (2020).

[3] Tanriover, I., Dereshgi, S.A., Aydin, K. Metasurface enabled broadband all optical edge detection in visible frequencies. *Nat Commun.* **14**, 6484 (2023).

[4] Zhao, M., Liang, X., Li, J., Xie, M., Zheng, H., Zhong, Y., Yu, J., Zhang, J., Chen, Z., Zhu, W. Optical phase contrast microscopy with incoherent vortex phase. *Laser Photon. Rev.* **16**, 2200230 (2022).

[5] Zhu, T., Lou, Y., Zhou, Y., Zhang, J., Huang, J., Li, Y., Luo, H., Wen, S., Zhu, S., Gong, Q., Qiu, M., Ruan, Z. Generalized spatial differentiation from the spin Hall effect of light and

its application in image processing of edge detection. *Phys. Rev. Appl.* **11**, 034043 (2019).

[6] Zhu, T., Huang, J., Ruan, Z. Optical phase mining by adjustable spatial differentiator. *Adv. Photonics.* **2**, 016001 (2020).

[7] Zhu, T., Guo, C., Huangm J., Wang, H., Orenstein, M., Ruan, Z., Fan, S., Topological optical differentiator. *Nat. Commun.* **12**, 680 (2021).

[8] Guo, C., Xiao, M., Minkov, M., Shi, Y., Fan, S. H. Photonic crystal slab Laplace operator for image differentiation. *Optica.* **5**, 251–256 (2018).

[9] Wang, Z., Hu, G., Wang, X., Ding, X., Zhang, K., Li, H., Burokur, S. N., Wu, Q., Liu, J., Tan, J., Qiu, C. W. Single-layer spatial analog meta-processor for imaging processing. *Nat. Commun.* **13**, 2188 (2022).

[10] Fu, W., Zhao, D., Li, Z., Liu, S., Tian, C., Huang, K. Ultracompact meta-imagers for arbitrary all-optical convolution. *Light.: Sci. Appl.* **11**, 62 (2022).

[11] Silva, A., Monticone, F., Castaldi, G., Galdi, V., Alù, A., Engheta, N. Performing Mathematical Operations with Metamaterials. *Science.* **343**, 160–163 (2014).

[12] Zhou, J., Qian, H., Zhao, J., Tang, M., Wu, Q., Lei, M., Luo, H., Wen,S., Chen, S., Liu, Z. Two-dimensional optical spatial differentiation and high-contrast imaging. *Natl Sci. Rev.* **8**, nwaa176 (2020).

[13] Zhou, Y., Zheng, H. Y., Kravchenko, I. I., Valentine, J. Flat optics for image differentiation. *Nat. Photonics.* **14**, 316–323 (2020).

[14] Kim, Y., Lee, G. Y., Sung, J., Jang, J., Lee, B. Spiral metalens for phase contrast imaging. *Adv. Fun. Mater.* **32**, 2106050 (2022).

[15] Zhou, Y., Wu, W., Chen, R., Chen, W., Chen, R., Ma, Y. Analog optical spatial differentiators based on dielectric metasurfaces. *Adv. Opt. Mater.* **8**, 1901523 (2019).

[16] Pan, D., Wan, L., Ouyang, M., Zhang, W., Potapov, A. A., Liu, W., Liang, Z., Feng, T., Li, Z. Laplace metasurfaces for optical analog computing based on quasi-bound states in the continuum. *Photon. Res.* **9**, 1758–1766 (2021).

[17] Cotrufo, M., Singh, S., Arora, A., Majewski, A., Alù, A. Polarization imaging and edge detection with image-processing metasurfaces. *Optica.* **10**, 1331–1338 (2023).

[18] Zhang, Y., Lin, P., Huo, P., Liu, M., Ren, Y., Zhang, S., Zhou, Q., Wang, Y., Lu, Y. Q., Xu, T. Dielectric metasurface for synchronously spiral phase contrast and bright-field imaging.

Nano Lett. **23**, 2991–2997 (2023).

[19] Cordaro, A., Kwon, H., Sounas, D., Koenderink, A. F., Alù, A., Polman, A. High-index dielectric metasurfaces performing mathematical operations. *Nano Lett.* **19**, 12 (2019).

[20] Cotrufo, M., Arora, A., Singh, S., Alù, A. Dispersion engineered metasurfaces for broadband, high-NA, high-efficiency, dual-polarization analog image processing. *Nat Commun.* **14**, 7078 (2023).

[21] Liu, Y., Huang, M., Chen, Q., Zhang, D. Single planar photonic chip with tailored angular transmission for multiple-order analog spatial differentiator. *Nat Commun.* **13**, 7944 (2022).

4. Is PB phase modulation required to realize the metalens?

Authors Reply: Thanks for the comment. The PB geometric phase usually depends only on the orientation angle of the nanostructure and is independent of the wavelength of the incident light. Therefore, it is very suitable for constructing broadband functional devices. For this reason, the complex amplitude modulation of our metalens is achieved using the PB phase. However, we also note that the PB phase is one of many choices in terms of BVMLs in this work. For example, we can design the devices using isotropic nanostructures, which usually induce the propagation phase and can enable a polarization-independent optical response. Further combining the geometric and propagation phases, we can also design polarization multiplexing devices to realize polarization control of different order differential operations in a single shot.

5. ω_l is the corresponding weight of each channel in Eq. (4). What is it for the 5 channels? How to determine and balance this value for various channels.

Authors Reply: Many thanks for the comment. The weight of each channel determines the light intensity of the channel and can be adjusted flexibly according to the practical application scenarios. In our imaging experiments, the weights of all five channels were set to 1/5 to ensure that each channel received the same light intensity.

6. A photo of the unstained limewood stem cell sample in the optical path is suggested to be given.

Authors Reply: Thanks for your constructive suggestion. We have added a photo of the unstained limewood stem cell sample in the optical path to the revised supplementary materials on Page 12.

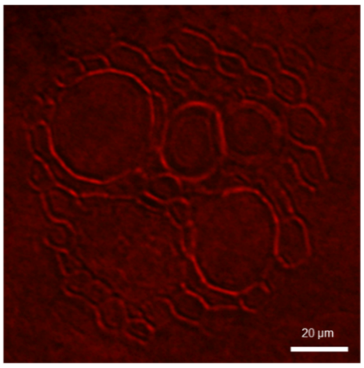

Figure R10 | Optical photographs of the unstained limewood stem cell sample.

7. Please give physical explanation for "higher-order differential operations have greater advantages in blocking low- to mid-frequency components" in Line 219-220.

Authors Reply: Thanks for the professional comment. According to the correspondence between the spatial differential operator and the transfer function, higher-order differential operations mean that its transfer function can exhibit a higher-order exponential relationship with the spatial frequency. Indeed, in our work, the coherent transfer function of the proposed BVML does satisfy the form of $t_l(k_r) \propto (\alpha f k_r/k_0)^l$ around $k_r = 0$, as shown in the theoretical curve and the fitting curve of Figure 1c-1f. Considering a lower spatial frequency interval, such as $|k_r| < 0.1k_0$, we can note that the coherent transfer function of the higher order differential operation shows even smaller values (the gray dashed line in Figure R11). As a result, higher-order differential operations can filter out more of the low- and mid-frequency components of the input light field. For clear expression, this sentence has been changed to "Higher-order differential operations have more significant advantages in filtering out low- and mid-frequency components" in line 221-222 of the revised manuscript.

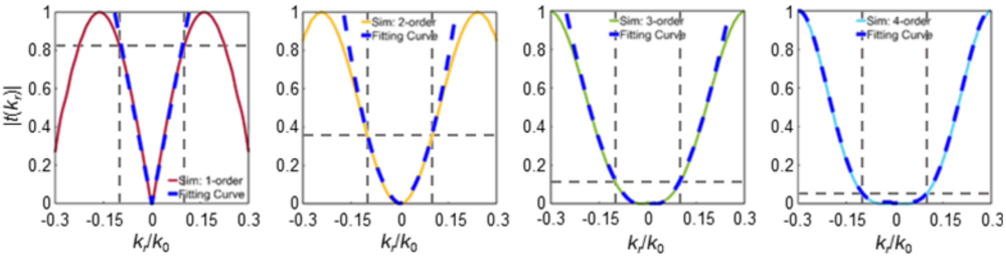

Figure R11 | The simulated CTF curves of different order BVMLs and the corresponding polynomial fitting curves of the same order. **a** The first-order, **b** The second-order, **c** The third-order, **d** The fourth-order.

8. It should be Fig.5e in Line 223.

Authors Reply: We thank the reviewer for pointing out this problem. It has been corrected to line 225 of the revised manuscript.

9. To apply the differentiation function of the method, the authors use the metalens for realizing edge detection. Are there any other applications for high order optical differentiation?

Authors Reply: Thanks for the comment. The proposed multifunctional BVML can synchronously perform multiple-order isotropic radial differential operations over broadband. Therefore, it is expected to enable massively parallel optical analog signal processing. In this work, we have demonstrated the capabilities of the device in edge detection and image sharpening. In addition, we envision that the synchronous multiple-order optical differentiation can also match the requirements for implementing complex operations and architectures, such as calculating the Taylor expansion of a mathematic input function, solving the differential equations with constant coefficients, and building optical convolutional neural networks.

REVIEWERS' COMMENTS

Reviewer #2 (Remarks to the Author):

The authors have addressed all the concerns, and I would like to recommend acceptance of the revised manuscript.

Reviewer #3 (Remarks to the Author):

After carefully reading the reply, I think that the present manuscript is clearly written. I have no more questions and would like to recommend publishing as present.

Reviewer #4 (Remarks to the Author):

The authors have answered all my questions in detail and made corresponding revision of the manuscript. I suggest this manuscript be considered to be accepted by Nature Communications.

1. The last line of Eq. (S6) is unnecessary and may be removed.

2. The last line of Eq. (S7) should be corrected as follows: $(-\boldsymbol{i})^{\boldsymbol{l}}\frac{\boldsymbol{exp(ik_0f)}}{\boldsymbol{i\alpha\lambda f}}\int_0^\infty\int_0^{2\pi}\boldsymbol{\delta}\left(\frac{\boldsymbol{k_0}}{\boldsymbol{f}}\boldsymbol{\rho}-\boldsymbol{\alpha}\right)\boldsymbol{exp}\left(\boldsymbol{ik_0}\frac{\boldsymbol{\rho^2}}{\boldsymbol{2f}}+\boldsymbol{il\phi}\right)\boldsymbol{e^{-ik_r\rho\cos(\varphi_k-\phi)}\rho}\mathbf{d}\boldsymbol{\phi}\mathbf{d}\boldsymbol{\rho}$ **according to Eq. (S6).**

Eq. (S8) should be revised as follows: $\boldsymbol{t_l}=(-\boldsymbol{i})^{\boldsymbol{l}}\frac{\boldsymbol{exp(ik_0f)}}{\boldsymbol{i\alpha\lambda f}}(-\boldsymbol{i})^{\boldsymbol{l}}\boldsymbol{exp(il\varphi_k)}\int_0^\infty\boldsymbol{\delta}\left(\frac{\boldsymbol{k_0}}{\boldsymbol{f}}\boldsymbol{\rho}-\boldsymbol{\alpha}\right)\boldsymbol{exp}\left(\boldsymbol{ik_0}\frac{\boldsymbol{\rho^2}}{\boldsymbol{2f}}\right)\boldsymbol{J_l(k_r\rho)\rho}\mathbf{d}\boldsymbol{\rho}=(-\mathbf{1})^{\boldsymbol{l}}\boldsymbol{f}\frac{\boldsymbol{exp(ik_0f)exp}\left(\boldsymbol{i}\frac{\boldsymbol{\alpha^2f}}{\boldsymbol{2k_0}}\right)}{\boldsymbol{i\lambda k_0^2}}\boldsymbol{J_l}\left(\frac{\boldsymbol{\alpha f}}{\boldsymbol{k_0}}\boldsymbol{k_r}\right)\boldsymbol{exp(il\varphi_k)}$. **Here** $\boldsymbol{\delta}\left(\frac{\boldsymbol{k_0}}{\boldsymbol{f}}\boldsymbol{\rho}-\boldsymbol{\alpha}\right)=\frac{\boldsymbol{f}}{\boldsymbol{k_0}}\boldsymbol{\delta}\left(\boldsymbol{\rho}-\frac{\boldsymbol{\alpha f}}{\boldsymbol{k_0}}\right)$**. Please check the above corrections for the two equations.**

3. It is recommended to cite other references related to multiple-order differentiation, such as Adv. Mater. 2023, 35, 2301505; and Nat. Commun. 2024, 15, 2237.

Reviewer #1:

1. The last line of Eq. (S6) is unnecessary and may be removed.

Authors Reply: Sincere thanks for this constructive comment. The last line of Eq. (S6) has been removed in revised supplementary Information.

2. The last line of Eq. (S7) should be corrected as follows: $(-i)^l \frac{exp(ik_0 f)}{i\alpha\lambda f} \int_0^\infty \int_0^{2\pi} \delta\left(\frac{k_0}{f}\rho - \alpha\right) exp\left(ik_0 \frac{\rho^2}{2f} + il\phi\right) \mathrm{e}^{-ik_r\rho\cos(\varphi_k - \phi)} \rho \mathrm{d}\phi\, \mathrm{d}\rho$ according to Eq. (S6).

Eq. (S8) should be revised as follows: $t_l = (-i)^l \frac{\exp(ik_0 f)}{i\alpha\lambda f} \cdot (-i)^l \exp(il\varphi_k) \int_0^\infty \delta\left(\frac{k_0}{f}\rho - \alpha\right) \exp\left(ik_0 \frac{\rho^2}{2f}\right) J_l(k_r\rho)\rho \mathrm{d}\rho = (-1)^l f \frac{\exp(ik_0 f)\exp\left(i\frac{\alpha^2 f}{2k_0}\right)}{i\lambda k_0^2} J_l\left(\frac{\alpha f}{k_0} k_r\right) \exp(il\varphi_k)$. Here $\delta\left(\frac{k_0}{f}\rho - \alpha\right) = \frac{f}{k_0}\delta\left(\rho - \frac{\alpha f}{k_0}\right)$. Please check the above corrections for the two equations.

Authors Reply: We are very grateful to the reviewer for his time and effort in reviewing the manuscript, and very much appreciate their insights. After careful checking, we have verified that the reviewer's results are completely correct, and we have revised Equations (S7) and (S8) in the supplementary Information.

3. It is recommended to cite other references related to multiple-order differentiation, such as Adv. Mater. 2023, 35, 2301505; and Nat. Commun. 2024, 15, 2237.

Authors Reply: Sincere thanks for this constructive comment. The relevant references have been added in the revised manuscript as ref. 45 and 46.

[45] Liang, X., Zhou, Z., Li, Z., Li, J., Peng, C., Cui, H., Wei, K., He, Z., Yu, S., Zheng, G. All-optical multiplexed meta-differentiator for tri-mode surface morphology observation. Adv. Mater. 35, 2301505 (2023).

[46] Deng, M., Cotrufo, M., Wang, J., Dong, J., Ruan Z., Alù, A., Chen, L. Broadband angular spectrum differentiation using dielectric metasurfaces. Nat Commun. 15, 2237 (2024).